Optical Cleanliness Measurement Methods for Aluminium Sheet Surfaces

Junjie Wang[1], Peter Andrews[1], Colin Butler[1], Eoghan McAlpine[1], Geoff Scamans[1] and Xiaorong Zhou[2].*

1 Innoval Technology Ltd., Beaumont Close, Banbury, Oxfordshire, OX16 1TQ, UK

2 School of Materials, The University of Manchester, Manchester, M13 9PL, UK

** Contact author telephone: +44 (0)1295702840, e-mail: junjie.wang@innovaltec.com*

Abstract

The cleaning of rolled aluminium surfaces is of critical importance for most applications and is of particular importance in automotive applications. The cleanliness of the sheet surface is mainly determined by the residual amount of the near-surface deformed layer on the alloy surface. This layer has nano-sized grains with their grain boundaries decorated and pinned by oxide particles and lubricant residues. The deformed layer reduces the reflectivity of the sheet or strip surface to visible light, particularly in the short wavelength range, resulting in a brownish appearance. Based on the optical characteristics of the deformed layer, the use of optical microscopy, spectrophotometry and colourimetry have been evaluated to provide a quantitative measurement of the level of cleanliness. These latter evaluations have been cross-checked by using scanning electron microscopy and transmission electron microscopy on ultramicrotomed cross-sections of aluminium sheet samples subjected to different level of cleaning to determine the amount of residual near-surface deformed layer.

Keywords: rolled aluminium sheet; surface cleaning; near-surface deformed layer; optical microscopy; spectrophotometry; colourimetry.

Introduction

The past decade has witnessed significant growth in the use of aluminium automotive body sheet (ABS) in the automotive industry to reduce vehicle weight for improved fuel economy and lower emissions from fossil fuelled vehicles, and extended driving range for electric vehicles. Major investments in automotive body sheet finishing lines, that commonly combine continuous heat treatment with the cleaning and pretreatment sections, have been made in the aluminium industry to keep pace with the fast-growing market. The cleaning process is used to prepare the sheet surface to apply the pretreatment. The cleaning involves chemical or electro-chemical etching of the sheet surface to remove the near-surface deformed layer which has been generated during hot and cold rolling due to the severe shear strain in the near-surface region and the interaction between the aluminium alloy surface and that of the steel rolls. The near-surface deformed layer has nano-sized grains with their grain boundaries decorated and pinned by rolled-in oxide particles and lubricant residues. The removal of the near-surface deformed layer is critical for the pretreatment to be successful in guaranteeing the long-term durability of adhesively bonded joints of automotive body structures [1] and in achieving good filiform corrosion resistance of the automotive sheet after painting [2-5]. However, excessive cleaning may cause problems, like copper re-deposition/enrichment [6] on the surface of copper containing aluminium alloys [7] such as AA6xxx alloys, which is detrimental to the corrosion resistance of the alloy. Excessive cleaning also increases the cost of maintenance of the cleaning section of the finishing line.

It is of great importance to evaluate the surface cleanliness of aluminium automotive body sheet, i.e. to determine the residual amount of the near-surface deformed layer after cleaning, so as to achieve surface quality control and to optimise the cleaning process in production. The current research method employed for this purpose is transmission electron microscopy (TEM) to examine cross-sectional specimens prepared by either ultramicrotomy or focused ion beam milling. The chemical composition, microstructure and thickness of the deformed layer can be analysed by TEM but the major drawbacks of this method are the very limited size of specimen that can be prepared and

examined each time and the cost and time involved. On cold rolled aluminium automotive body sheet with a thickness between 0.8 and 3.0 mm, the deformed layer usually has a maximum thickness in the range of several hundred nanometres to several micrometres and is not continuous on the sheet surface. Therefore, the cross-sectional electron microscopic examination might not reveal the real amount of the deformed layer on the sheet surface due to the variability across the surface. High resolution low accelerating voltage scanning electron microscopy has the capability of imaging the ultrafine grains directly on the rolled aluminium alloy surface by the channelling contrast of backscattered electrons [8, 9]. Nevertheless, the effectiveness of this latter technique is significantly affected by the topography of the rolled surface, especially for aluminium automotive body sheet rolled with electro-discharge textured (EDT) rolls. The surface roughness Ra is commonly in the range of 0.3 - 0.6 μm for mill finish surface and 0.7 - 1.3 μm for EDT surface. Elemental depth profiling techniques, such as GDOES, AES, XPS and SIMS, etc., have been used to analyse the depth profile of different elements in the deformed layer of rolled aluminium alloys but, again, the accuracy of these techniques has been significantly affected by the surface roughness of aluminium automotive body sheet.

All the above described techniques are based on characterising the unique, nano-grained microstructure and/or the altered chemical composition of the deformed layer. As an alternative, a combination of progressive alkaline etching and total reflectance measurement has been proposed as a technique which can be used to estimate the thickness of the deformed layer on rolled aluminium alloys [10-14]. This technique is based on the optical characteristics of the deformed layer which can reduce the reflectivity of the rolled aluminium alloy sheet surface to visible light. Another optical characteristic of the deformed layer is that it reduces the reflectivity to visible light more in the short wavelength range, resulting in a red shift in the total reflectance spectra [15]. It is probable that the rolled-in oxide particles in the deformed layer of aluminium alloy sheet are responsible for these optical characteristics [10-12, 15-17]. The dielectric aluminium oxide has a total reflectance of approximately 7 % [18] over the visible wavelength range while that of pure metallic aluminium is 91-92 % [19]. A mixture of these two materials leads to a composite reflectivity value. Studies on a

magnetron sputtered layer of aluminium and aluminium oxide on a pure aluminium substrate found that the red shift was associated with the presence of aluminium oxide in the sputtered layer. The level of red shift increases with the aluminium oxide content in the sputtered layer up to ~ 30 wt. % [16, 20].

In the present work, the optical characteristics of the deformed layer on rolled aluminium sheets have been further investigated. Different optical approaches, including microscopy, spectrophotometry and colourimetry have been evaluated to provide a quantitative measurement of the level of cleanliness. These observations have been cross-checked by using scanning electron microscopy (SEM) and transmission electron microscopy (TEM) on ultramicrotomed cross-sections of aluminium sheet samples subjected to different levels of cleaning to determine the amount of residual deformed layer.

Experimental

Sheet samples of a variety of commercial aluminium alloys with different tempers, gauges and surface textures were used in the present work, as shown in Table 1. All samples were cut to dimensions of 80 mm by 25 mm and then degreased using hexane to remove the rolling lubricant from the surface. Samples were then etched in 5 wt. % NaOH solution at 60 °C for different times as shown in Table 2, followed by de-smutting process in 30 vol. % HNO_3 solution at ambient temperature. The alkaline etching and corresponding acid de-smutting procedures were applied to simulate the aluminium sheet cleaning process used in industrial cleaning applications.

The evolution of surface appearance of the samples subjected to different level of cleaning was examined using an optical microscope with the white balance corrected to show the real colour of the sample surface. A spectrophotometer equipped with an integrating sphere with a sample port diameter of 10.32 mm (area 83.6 mm^2) was used to measure the total reflectance of the sample surface to visible light, i.e. wavelength range 380 – 780 nm. The L*a*b* colour space lightness value L* and

chromaticity values a* and b* of the sample surface were measured using colourimetry. Cross sections of selected sheet samples subjected to different level of cleaning were prepared using ultramicrotomy and examined using scanning electron microscopy and transmission electron microscopy to determine the existence and the amount of residual near-surface deformed layer.

Results and discussion

Figure 1 shows the visual appearance of the surface of a 1.5 mm gauge AA5182-O automotive sheet with different levels of cleaning. After hexane degreasing, the sheet surface had a dark and brown appearance. Micro-cracks transverse to the rolling direction on the sheet surface were found to be filled with a mixture of aluminium fines and lubricant residues, as indicated by arrows in Figure 1a. After 2 seconds of alkaline etching and then de-smutting the majority of the aluminium fines and lubricant residue were removed from the transverse cracks, exposing the bright and silver white underlying bulk alloy, as indicated by the arrows in Figure 1b. A large fraction of the sheet surface was still brown. With an increased level of cleaning, the original brown surface was progressively replaced by the freshly exposed bulk alloy. The association of the transverse micro-cracks with the brown patches is readily observable on the sheet surface, as shown in Figure 1c-f. All brown patches and micro-cracks disappeared from the sheet surface after 60 seconds of alkaline etching, leaving a silver white sheet surface. The simultaneous disappearance of the micro-cracks and the brown patches demonstrates that the depth of these micro-cracks was of the same order as the thickness of the brown patches. Prolonged cleaning did not change the colour of the sheet surface any further once all brown patches were removed. Scalloped features started to appear on the cleaned sheet surface and the size of these scalloped features grew with alkaline etching time. Such observations are typical for alkaline etching and HNO_3 de-smutting of aluminium alloys [21].

Figure 2 shows scanning electron micrographs and corresponding EDX maps of the 1.5 mm gauge AA5182-O automotive sheet surface which was subjected to 10 seconds of alkaline etching and acid

de-smutting. Transverse micro-cracks are readily observable from the secondary election micrograph (Figure 2a). These cracks are associated with the dark patches in the backscattered electron micrograph (Figure 2b), which correspond to the brown patches in the optical micrographs in Figure 1. The EDX mapping analysis at an accelerating voltage of 8 kV showed the enrichment of oxygen and magnesium in the dark patches, as shown in Figure 2d and e, indicating the enrichment of magnesium oxide. Aluminium oxide is also present in the deformed layer [22]. Enrichment of carbon (Figure 2f) suggests the incorporation of lubricant residue in the dark patches.

The secondary electron micrograph in Figure 3a shows the cross-sectional microstructure in the near-surface region of an ultramicrotomed block taken from the location indicated by the dashed line in Figure 2b. The remnant of a near-surface deformed layer patch with microstructure different from the bulk alloy is evident. The maximum thickness of the layer is approximately 3 μm. Oxide particles were found in the deformed layer, as indicated by solid arrows in Figure 3b. The dark appearance of these particles in the backscattered electron micrograph indicates the presence of elements with a relatively small atomic number compared to aluminium, thus, exhibiting the distribution of oxide particles. This is consistent with the enrichment of oxygen and magnesium in this region as shown in Figure 2. A high population density of AlFeMnSi particles, appearing as bright spots in the backscattered electron micrograph, was found in the deformed layer due to their preferential precipitation during the thermo-mechanical processing and the final annealing [23]. The results show that the brown patches on the 1.5 mm gauge AA5182-O automotive sheet surface are patches of the near-surface deformed layer. This finding therefore enables the examination of the deformed layer on aluminium sheet surfaces to be determined using conventional optical microscopes. Observation using an optical microscope at a magnification of 500x or 1000x works best to examine the deformed layer. This approach has many advantages, including relatively large sampling area compared to electron microscopy, simple sample preparation, rapid observation and data collection, more use of conventional equipment and low cost, etc. The relatively large examined area is important for a meaningful quantitative analysis of the coverage of the deformed layer on rolled aluminium sheet surfaces.

Transmission electron micrographs of ultramicrotomed cross-sections taken randomly from the 1.5 mm gauge AA5182-O automotive sheet which was subjected to different level of cleaning are shown in Figure 4. On the hexane degreased surface, a nano-grained deformed layer with thickness varying from tens of nanometres to a maximum of approximately 1.8 μm was found (Figure 4a). This is smaller than the 3 μm thickness of the deformed layer found on the sheet surface shown in Figure 2, which was subjected to 10 seconds of alkaline etching and acid de-smutting. Micro-cracks can be seen within the deformed layer, corresponding to the transverse cracks within the brown deformed layer patches on the sheet surface, as shown in Figure 1a. The micro-cracking within the deformed layer is promoted by the high population density of oxide particles at the grain boundaries within the deformed layer which therefore has a relatively low ductility compared to the bulk alloy [24]. Micro-cracks transverse to the rolling direction occur within the deformed layer once it cannot accommodate the deformation. During a multi-pass warm and cold rolling process, the micro-cracks continue growing and the underlying ductile bulk alloy is extruded into the micro-cracks, eventually separating the deformed layer into discrete patches, as shown in Figure 1. After 5 seconds of alkaline etching and acid de-smutting, the deformed layer is partially removed from the sheet surface, as shown in Figure 1c. However, the maximum thickness of the residual deformed layer was still about 1.8 μm on the examined specimen (Figure 4b). After 10 seconds of alkaline etching and acid de-smutting, the residual deformed layer was further removed, but the maximum thickness was still approximately 1.8 μm on the examined specimen (Figure 4c), confirming the disadvantage of the limited TEM examination area. Areas free of deformed layer were easily found on the specimen after 10 seconds of alkaline etching and acid de-smutting (Figure 4d), which is the same as the sheet surface subjected to 60 seconds of alkaline etching and acid de-smutting where all the deformed layer was removed (Figure 4e). Only a uniform, naturally formed oxide film with a thickness of approximately 5 nm was present on the cleaned surface, as shown in Figure 4f and this confirms the risk of deriving conclusions on the existence of deformed layer on a sheet surface due to different TEM sampling locations. The same risk applies to cross-sectional SEM examinations.

The reflectivity in the visible light range (380-780nm) of the 1.5 mm gauge AA5182-O automotive sheet surface subjected to different levels of cleaning is shown in Figure 5. Figure 5a shows the total reflectance (TR) of the sheet surface as a function of the incident visible light wavelength. The hexane degreased surface (etched 0 second) showed a low TR value of 32 % at 380 nm, which is the blue end of the visible light spectrum. The TR value increased with wavelength and reached 59 % at 780 nm, which corresponds to the red end of the visible light spectrum. The relatively high value of the TR profile at the red end, i.e. a red shift, is consistent with the brown appearance of the sheet surface. On progressive alkaline etching for up to 5 seconds, the TR did not change much, but the level of red shift reduced gradually. The TR then increased progressively and the level of red shift further decreased with alkaline etching time until 60 seconds when all the deformed layer was removed from the sheet surface. Further etching did not change the TR or the level of red shift. Figure 5b shows a plot of integrated TR values over the wavelength range 380 – 780 nm as a function of the alkaline etching time. The integrated TR value of the hexane degreased surface was 49 %, which did not change much with 5 seconds of alkaline etching. Further, the integrated TR value increased and reached 83 % after 60 seconds of alkaline etching. The integrated TR value was then constant with further alkaline etching. The TR profiles and the integrated TR values for different level of cleaning were consistent with the progressive disappearance of the deformed layer on the sheet surface as recorded by optical microscopy. The total reflectance measurement using spectrophotometry is therefore eminently suitable for quantitative analysis of the cleanliness of aluminium sheet surfaces.

Figure 6 shows the colourimetry results obtained on the 1.5 mm gauge AA5182-O automotive sheet surface subjected to different level of cleaning. The lightness value L* shows a very similar profile to the integrated TR since both are basically the same and reflect the brightness of the examined sheet surfaces. The chromaticity values a* and b* together represent the colour of the sheet surface. In the a*, b* chromaticity diagram, +a* is the red direction and -a* is the green direction, +b∗ is the yellow direction and -b∗ is the blue direction. As shown in Figure 6, the a* value gradually decreased from around 1.6 at 2 seconds of alkaline etching to about -0.2 at 60 seconds of alkaline etching and then

levelled off with prolonged etching time. The b* value showed a progressive decrease from 9.7 to 0 during the first 60 seconds of alkaline etching and then levelled off.

In a portion of the a*, b* chromaticity diagram, the chromaticity of all the examined aluminium sheet surfaces were plotted, as shown in Figure 7. The chromaticity plot of the hexane degreased surface of the 1.5 mm gauge AA5182-O automotive sheet surface is located in the yellow-brown domain of the chromaticity diagram, which is consistent with the optical microscopic observation of the brown appearance of the deformed layer. With the progression of cleaning, the chromaticity plot moved linearly towards the centre of the chromaticity diagram, indicating that the chromaticity of the sheet surface was virtually unchanged with progressive cleaning, but the saturation of the brown colour of the sheet surface decreased gradually. The saturation $\sqrt{(a^{*2} + b^{*2})}$ can be calculated from the chromaticity values. The decrease in saturation can be explained by the decreasing amount of deformed layer on the sheet surface with progressive cleaning. Any residual deformed layer retained the brown appearance until it had been removed. However, once the saturation was reduced to a certain level, i.e. ~ 4, the chromaticity of the sheet surface was not visually observable [18]. For aluminium sheet or foil applications where surface visual chromaticity appearance is critical and this can be used as a control value to determine what level of cleanliness should be achieved. After 60 seconds of alkaline cleaning, the chromaticity plot of the sheet surface reached the centre of the chromaticity diagram which is achromatic. The sheet surface appeared as silver white at this point as shown in Figure 1e. The chromaticity plots of AA5182 (EDT), AA6016 (EDT) and AA3103 (mill finish) sheets are located in the same yellow-brown domain as the 1.5 mm gauge AA5182-O (mill finish) automotive sheet and show similar linear trend towards the centre of the chromaticity diagram with progressive cleaning. This demonstrates that the deformed layer on different rolled aluminium alloys has a similar brown colour with only minor variations, regardless of changes in alloy composition and the different surface textures, i.e. mill finish and EDT. The correlation between the chromaticity values a* and b* of the aluminium alloy sheet surface and the amount of residual deformed layer on sheet surface shows the possibility of using colourimetry to quantitatively analyse the cleanliness of the sheet surface. Due to the linear relationship between a* and b* values, only one

of them is required for the analysis. The chromaticity of the deformed layer on aluminium sheet surface is closer to the b* coordinate than the a* coordinate on the a*, b* chromaticity diagram. The change in b* value upon different level of cleaning is larger than that of a* value. Therefore, the b* value is preferred and the use of b* value rather than a* value can decrease the level of error in measurements.

Figure 8a shows the integrated TR profiles of all examined aluminium alloys sheet surfaces with different levels of cleaning. All the TR profiles show a similar ascending trend until a constant value of integrated TR has been reached after a certain alkaline etching time for each material. The integrated TR of hexane degreased surface for these alloys has a range of values, indicating different levels of deformed layer coverage. The hexane degreased 0.8 mm gauge AA5182-O automotive sheet surface shows a higher integrated TR value than that of the hexane degreased 1.5 mm gauge AA5182-O automotive sheet. The integrated TR of the 0.8 mm gauge AA5182-O automotive sheet surface reached a constant value after 20 seconds of alkaline etching when all the deformed layer was removed, while that of the 1.5 mm gauge AA5182-O automotive sheet surface required 60 seconds, indicating a thicker deformed layer. These two AA5182 materials were from different hot band sources. The possible reason for this difference is due to the original amount of deformed layer after breakdown rolling and the total reduction in cold rolling, etc. The deformed layer on aluminium alloy sheets is mainly generated during hot rolling. High aspect ratio rolling, high rolling speed and rough and worn roll surfaces result in a relatively thick deformed layer on hot rolled aluminum alloy surface [25]. Cold rolling spreads the deformed layer over a larger surface area and disrupts its continuity, resulting in it being randomly distributed as discrete patches on the alloy surface [24, 26]. A larger total reduction in cold rolling spreads the deformed layer over a larger surface area, which either reduces the percentage of coverage or the thickness of the deformed layer on the alloy surface: this was confirmed by the reflectivity profiles of the two AA3103 sheets. The 1.2 mm gauge AA3103-H12 sheet required about 10 seconds of alkaline etching to remove all the deformed layer and reach the

highest integrated TR value, while the 0.5 mm gauge AA3103-H18 sheet only required about 5 seconds of etching.

Figure 8b shows the chromaticity b* value profiles of all examined aluminium alloys sheet surfaces with different levels of cleaning. All the profiles show a similar descending trend until a constant b* value has been reached at certain alkaline etching time for each material. Similar to the integrated TR, the b* value of the hexane degreased also reflects different levels of deformed layer coverage. The smaller thickness and surface coverage of the deformed layer on the 0.8 mm gauge AA5182-O automotive sheet compared to the 1.5 mm gauge AA5182-O automotive sheet are well represented by the b* value profiles. The b* value profiles of the two AA3103 sheets show a shorter alkaline etching time was required to remove all the deformed layer on the 0.5 mm gauge sheet than the 1.2 mm gauge sheet, which matches the integrated TR results.

In rolled aluminium alloys, both Al_2O_3 and MgO particles were found in the deformed layer [22]. Previous studies [18, 20] revealed the impact of Al_2O_3 particles on optical properties, i.e. lower reflectivity and a red shift, of a magnetron sputtered aluminium layer, which was a simulation of the deformed layer on aluminium alloys. MgO has similar optical properties to Al_2O_3. Both oxides are transparent and have a similar refractive index of about 1.7 within the visible wavelength range. Therefore, it is reasonable to suggest that MgO can also lower reflectivity and promote a red shift. It should be noted that there may be different stoichiometries of aluminium oxides and magnesium oxides in the deformed layer, which may have different optical properties. Magnesium is more prone to oxidation than aluminium since the Gibbs free energy for oxidation of magnesium per equivalent ($\Delta G°/eq$) is more negative than that of aluminium. In addition, magnesium segregates towards the alloy surface by diffusion during heat treatment and thermo-mechanical processing. The level of magnesium segregation is determined by the magnesium concentration and the thermal history of the alloy. Assuming the same thermal history, the oxide film formed on the surface of high magnesium

containing aluminium alloys is usually thicker than that of low- or non-magnesium containing aluminium alloys. As a result, there are more oxide particles available to be incorporated into the near-surface region in high magnesium containing aluminium alloys due to the alloy surface and roll surface interaction during rolling. This contributes to the generation of a larger amount of deformed layer and a higher population density of oxide particles in the deformed layer, leading to a lower reflectivity and a stronger red shift, i.e. higher saturation of the brown colour of the sheet surface. This is confirmed by the saturation of the brown colour of the hexane degreased aluminium alloys examined, although the thermal history of these alloys were not exactly the same. For aluminium alloys virtually free of magnesium, like AA3103, the saturation of the brown colour is very low and may not be visually observable. In this case, total reflectance measurement using spectrophotometry and chromaticity measurement using colourimetry work better than optical microscopic examination for quantitative analyses.

Conclusions

1. The near-surface deformed layer generated on hot and then cold rolled aluminium alloys is present as brown patches on the alloy surface. The near-surface deformed layer on aluminium alloys with different tempers, gauges, surface textures and chemical compositions has a similar chromaticity, i.e. brown colour.
2. Upon progressive cleaning, chromaticity of the sheet surface is virtually unchanged. The saturation of the brown colour decreases progressively due to the gradual removal of the near-surface deformed layer.
3. Cross-sectional TEM and SEM examinations are not suitable for accurate determination of the distribution of deformed layers on aluminium alloy sheet surfaces due to the limited size of sample that can be prepared and examined each time.
4. The residual level of deformed layers on a rolled aluminium alloy, which is a direct indication of the effectiveness of the cleaning process, can be quantitatively assessed using optical microscopy,

total reflectance measurements with spectrophotometry and chromaticity measurements with colourimetry.

5. For aluminium alloy sheet or foil products the surface visual appearance is important and the critical value of brown colour saturation $\sqrt{(a^{*2} + b^{*2})} = \sim 4$ can be used as a control value to determine the level of cleanliness to be achieved.
6. For low magnesium aluminium alloys, like AA3103, the saturation of the brown colour is low and may not be visually observable. In this case, total reflectance measurements and chromaticity measurements work better than optical microscopy for quantitative analyses.

Acknowledgements

The authors wish to thank Innoval Technology Ltd. for permission to publish this work.

References

1. Scamans GM. Cleaning and pretreatment of aluminium sheet to remove deformed surface layers. Light Met Age 2016;December:12-18.
2. Scamans GM, Afseth A, Thompson GE, Zhou X. Thermomechanical Proceessing Induced Corrosion of Aluminium Alloy Sheet. in 2nd International Syposium on Aluminium Surface Science and Technology. Manchester, UK. ATB Metall 2000;40:9-16.
3. Scamans GM, Afseth A, Thompson GE, Liu Y, Zhou X. Corrosion of Painted Aluminium Sheet. Mater Sci Forum 2006;519-521:647-654.
4. Nordlien JH, Davenport AJ, Scamans GM. Filiform Corrosion Studies of Analogue Automotive Model Alloys Based on Super-purity Aluminium. in 2nd International Syposium on Aluminium Surface Science and Technology. Manchester, UK. ATB Metall 2000;40:107-112.
5. Liu Y, Zhou X, Thompson GE, Hashmoto T, Scamans GM, Afseth A. Precipitation in an AA6111 aluminium alloy and cosmetic corrosion. Acta Mater 2007;55:353-360.
6. Liu Y, Colin F, Skeldon P, Thompson GE, Zhou X, Habazaki H, Shimizu K. Enrichment factors for copper in aluminium alloys following chemical and electrochemical surface treatments. Corros Sci 2003;45:1539-1544.
7. Muster TH, Hughes AE, Thompson GE. eds. Copper distributions in aluminum alloys. Corrosion research trends, ed. I.S.Wang. 2007, Nova Science Publisher: New York.
8. Scamans GM, Frolish MF, Rainforth WM, Zhou Z, Liu Y, Zhou X, Thompson GE. The ubiquitous Beilby layer on aluminium surfaces. Surf Interface Anal 2010;42:175-179.
9. Liu B, Zhou X. The impact of machining on the corrosion behaviour of AA7150-T651 aluminium alloy. Mater Sci Forum 2014;794-796:217-222.
10. Premendra, Chen JH, Tichelaar FD, Terryn H, deWit JHW, Katgerman L. Optical and transmission electron microscopical study of the evolution of surface layer on recycled aluminium along the rolling mills. Surf Coat Technol 2007;201:4561-4570.

11. Buytaert G, Terryn H, Van Gils S, Kernig B, Grzemba B, Mertens M. Investigation of the (sub)surface of commercially pure rolled aluminium alloys by means of total reflectance, r.f. GDOES, SEM/EDX and FIB/TEM analysis. Surf Interface Anal 2006;38:272-276.
12. Buytaert G, Kernig B, Brinkman HJ, Terryn H. Influence of surface pre-treatments on disturbed rolled-in subsurface layers of aluminium alloys. Surf Coat Technol 2006;201:2587-2598.
13. Buytaert G, Terryn H, Van Gils S, Kernig B, Grzemba B, Mertens M. Study of the near-surface of hot- and cold-rolled AlMg0.5 aluminium alloy. Surf Interface Anal 2005;37:534-543.
14. Buytaert G, Terryn H, Van Gils S, Kernig B, Grzemba B. Analytical Study of the Surface of Hot Rolled Al Alloys. in 3rd International Syposium on Aluminium Surface Science and Technology. Bonn, Germany. ATB Metall 2003;43:475-481.
15. Lindseth I, Bardal A, Spooren R. Reflectance measurements of aluminium surfaces using integrating spheres. Optics and Lasers in Engineering 1999;32:419-435.
16. Van Gils S, Dimogerontakis Th, Buytaert G, Stijns E, Terryn H, Skeldon P, Thompson GE, Alexander MR. Optical properties of magnetron-sputtered and rolled aluminum. J Appl Phys 2005;98:083505.
17. Lindseth I, Bardal A. Identification of Surface Morphological Features That Cause Enhanced Optical Absorption in Rolled Aluminium Metals. in 2nd International Syposium on Aluminium Surface Science and Technology. Manchester, UK. ATB Metall 2000;40:35-40.
18. Van Gils S, Shedding Light on Metals: Use of Optical Techniques for Surface Analysis and Appearance Characterisation of Aluminium. PhD thesis. 2004, Vrjie Universiteit Brussel, Brussels.
19. Palik ED, ed. Handbook of optical constants of solids, vol 1. London: Academic Press; 1998.
20. Li K, Origins and evolution of near-surface microstructures and their influence on the optical property of AA3104 aluminium alloy, PhD thesis. 2013, The University of Manchester, Manchester.
21. Rivett B, Koroleva EV, Garcia-Garcia FJ, Armstrong J, Thompson GE, Skeldon P. Surface topography evolution through production of aluminium offset lithographic plates. Wear 2011;270:204-217.
22. Fishkis M, Lin JC. Formation and evolution of a subsurface layer in a metalworking process. Wear 1997;206:156-170.
23. Afseth A, Nordlien JH, Scamans GM, Nisancioglu K. Effect of heat treatment on filiform corrosion of aluminium alloy AA3005. Corros Sci 2001;43:2093-2109.
24. Wang J, Zhou X, Thompson GE, Hunter JA, Yuan Y. Delamination of near-surface layer on cold rolled AlFeSi alloy during sheet forming. Mater Charact 2015;99:109-117.
25. Liu Y, Frolish MF, Rainforth WM, Zhou X, Thompson GE, Scamans GM, Hunter JA. Evolution of near-surface deformed layers during hot rolling of AA3104 aluminium alloy. Surf Interface Anal 2010;42:180-184.
26. Zhou X, Liu Y, Thompson GE, Scamans GM, Skeldon P, Hunter JA. Near-Surface Deformed Layers on Rolled Aluminum Alloys. Metall Mater Trans A 2011;42:1373-1385.

Table 1. Temper, gauge, surface texture and chemical composition of aluminium alloys investigated.

Alloy	Temper	Gauge (mm)	Surface texture	Chemical compositions (wt. %)				
				Si	Fe	Cu	Mn	Mg
AA5182	O	1.5	MF	0.16	0.24	0.04	0.33	4.25
AA5182	O	0.8	EDT	0.13	0.25	0.07	0.42	4.20
AA6016	T4P	1.0	EDT	1.16	0.24	0.11	0.09	0.52
AA3103	H12	1.2	MF	0.2	0.57	0.002	1.07	0.002
AA3103	H18	0.5	MF	0.19	0.6	0.016	1.17	0.009

Table 2. Schedule for progressive cleaning

Cleaning process	**Duration (s)**							
Alkaline etching	1	2	5	10	20	30	60	120
Acid de-smutting	5	5	10	30	30	30	30	30

Figure 1. Optical micrographs of 1.5mm gauge AA5182-O automotive sheet surface subjected to different level of alkaline etching: (a) hexane degreased, no etching; (b) 2 s; (c) 5 s; (d) 10 s; (e) 20 s; (f) 30 s; (g) 60 s; (h) 120 s.

Figure 2. Electron micrographs and corresponding EDX maps (accelerating voltage: 8 kV) of 1.5mm gauge AA5182-O automotive sheet surface subjected to 10 seconds of alkaline etching: (a) secondary electron micrograph; (b) backscattered electron micrograph; (c) aluminium map; (d) oxygen map; (e) magnesium map; (f) carbon map.

Figure 3. (a) secondary electron micrograph of an ultramicrotomed block taken from the location indicated by the dashed line in Figure 2b; (b) backscattered electron micrograph of the framed area in (a).

Figure 4. Transmission electron micrographs of ultramicrotomed cross sections of the near-surface region of 1.5mm gauge AA5182-O automotive sheet surface subjected to different time of alkaline etching: (a) hexane degreased, no etching; (b) 5 s; (c) 10 s, region with deformed layer; (d) 10 s, region free of deformed layer; (e) 60 s; (f) 60 s, at increased magnification.

Figure 5. Reflectivity of 1.5mm gauge AA5182-O automotive sheet surface subjected to different level of alkaline etching: (a) surface total reflectance as a function of visible light wavelength; (b) integrated total reflectance as a function of alkaline etching time.

Figure 6. Lightness value L* and chromaticity values a* and b* of 1.5 mm gauge AA5182-O automotive sheet surface as a function of the alkaline etching time.

Figure 7. A portion of a*, b* chromaticity diagram with a constant L* value, showing the chromaticity of a variety of aluminium sheet surfaces subjected to different level of cleaning.

Figure 8. Reflectivity of aluminium alloys subjected to different level of alkaline etching: (a) integrated total reflectance; (b) profiles of chromaticity value b*.

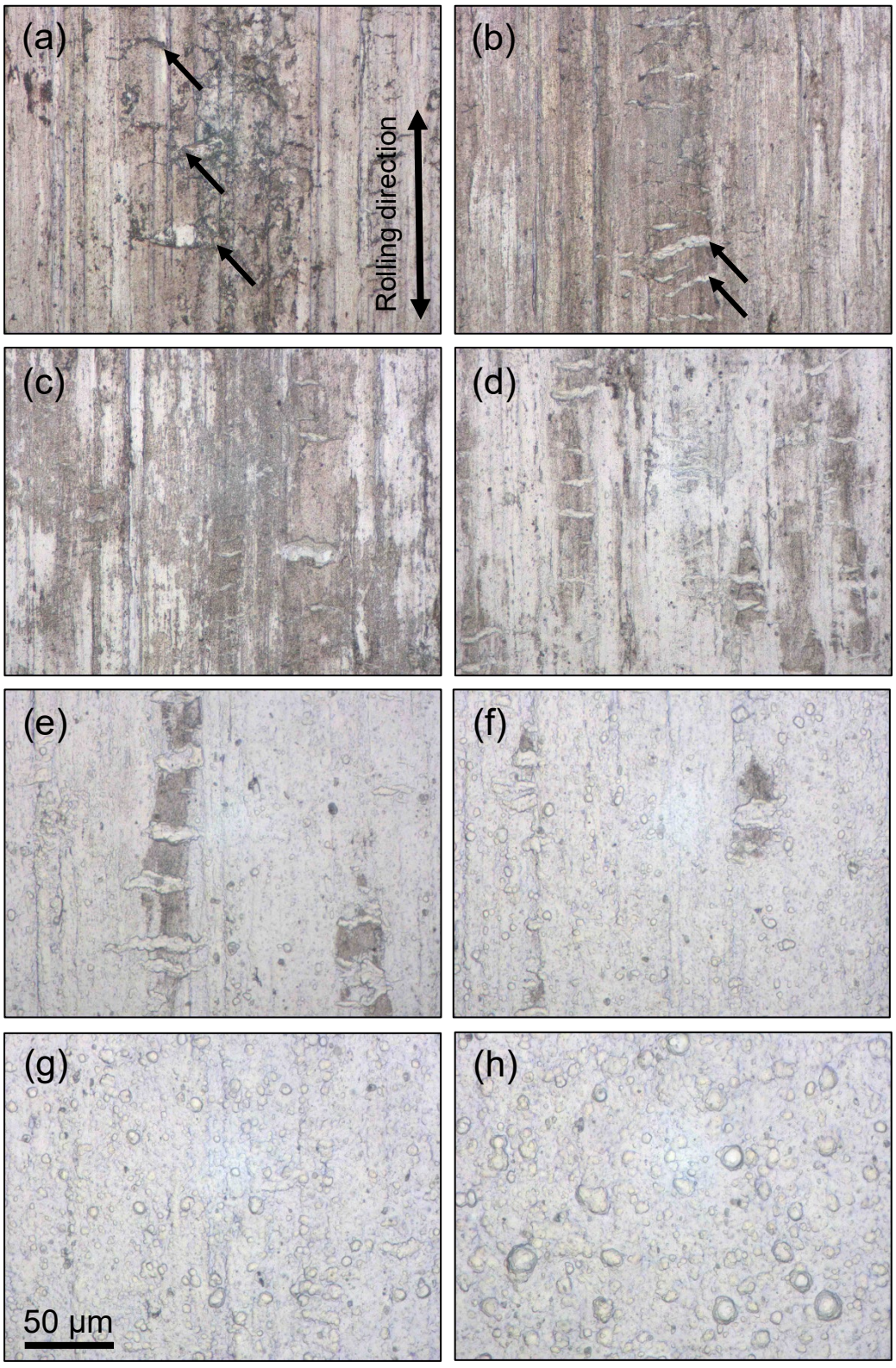

Figure 1. Optical micrographs of 1.5mm gauge AA5182-O automotive sheet surface subjected to different level of alkaline etching: (a) hexane degreased, no etching; (b) 2 s; (c) 5 s; (d) 10 s; (e) 20 s; (f) 30 s; (g) 60 s; (h) 120 s.

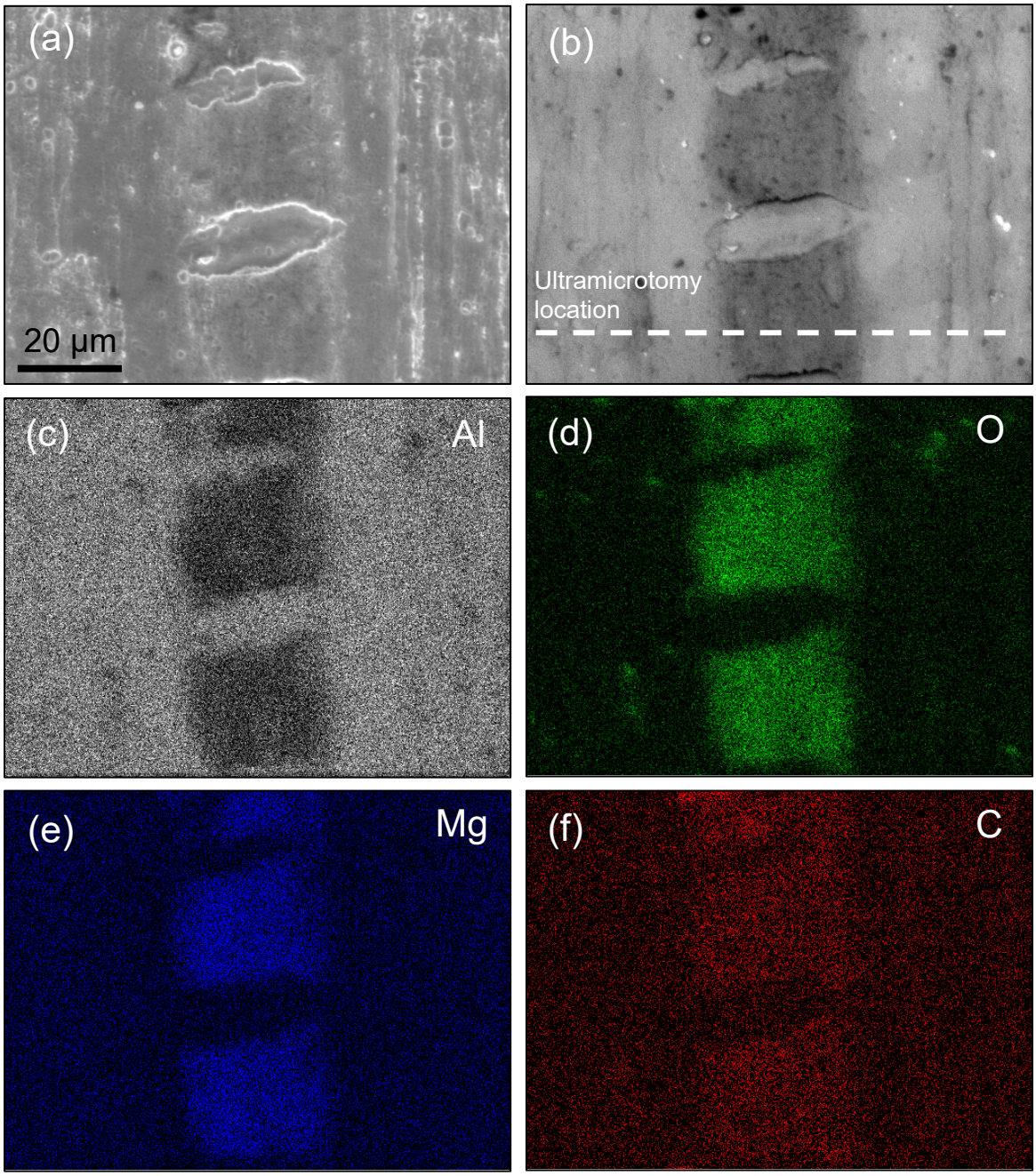

Figure 2. Electron micrographs and corresponding EDX maps (accelerating voltage: 8 kV) of 1.5mm gauge AA5182-O automotive sheet surface subjected to 10 seconds of alkaline etching: (a) secondary electron micrograph; (b) backscattered electron micrograph; (c) aluminium map; (d) oxygen map; (e) magnesium map; (f) carbon map.

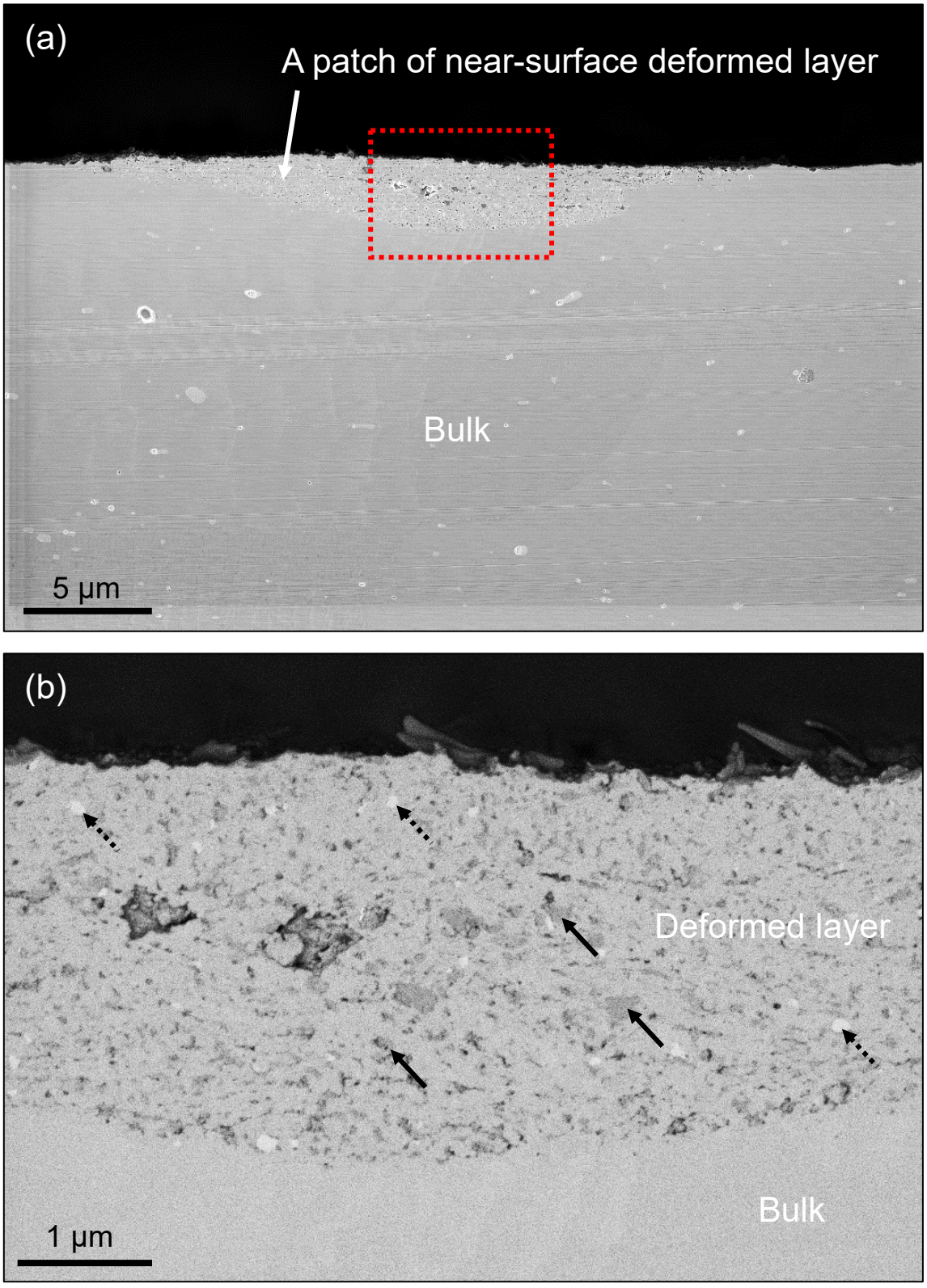

Figure 3. (a) secondary electron micrograph of an ultramicrotomed block taken from the location indicated by the dashed line in Figure 2b; (b) backscattered electron micrograph of the framed area in (a).

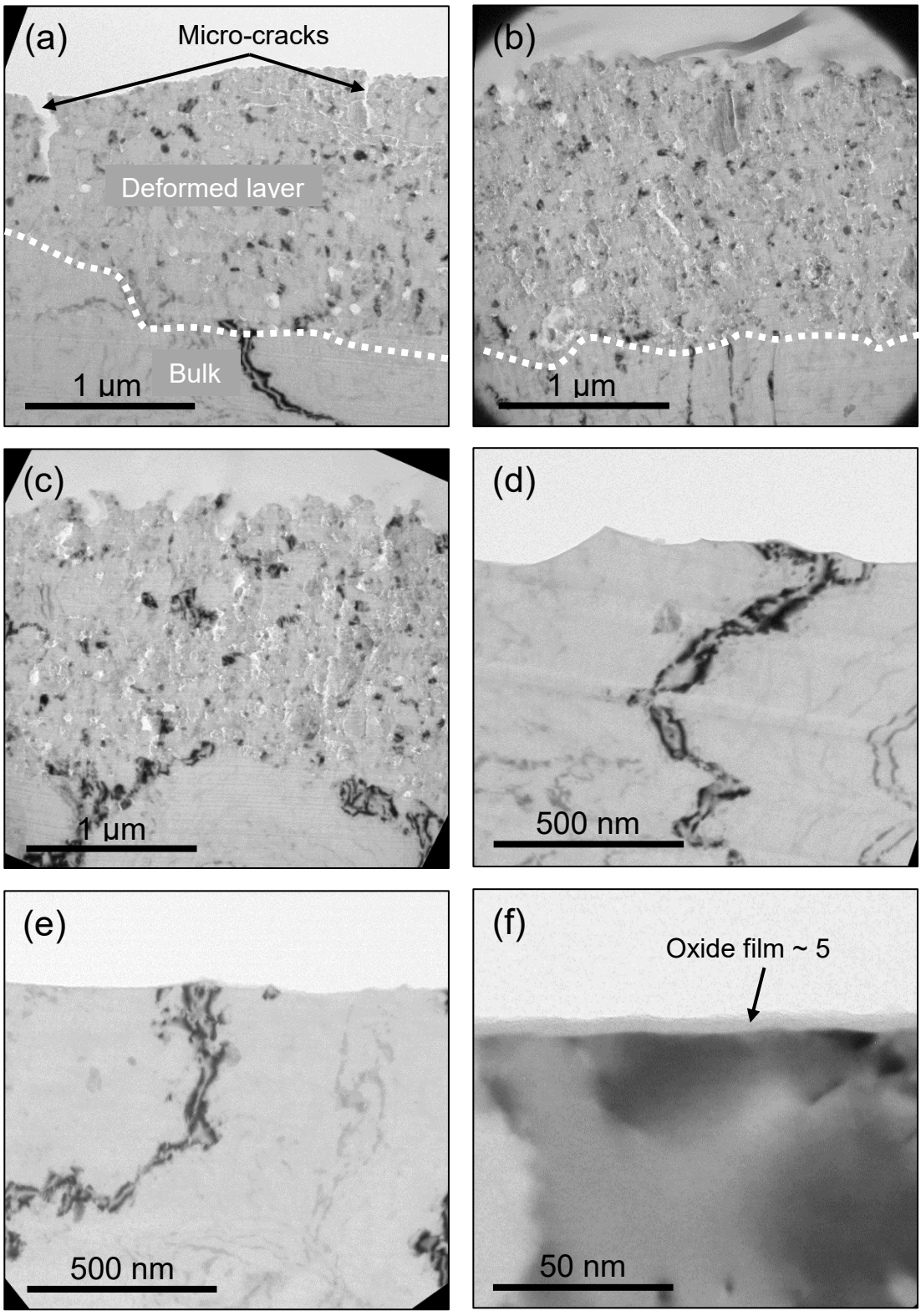

Figure 4. Transmission electron micrographs of ultramicrotomed cross sections of the near-surface region of 1.5mm gauge AA5182-O automotive sheet surface subjected to different time of alkaline etching: (a) hexane degreased, no etching; (b) 5 s; (c) 10 s, region with deformed layer; (d) 10 s, region free of deformed layer; (e) 60 s; (f) 60 s, at increased magnification.

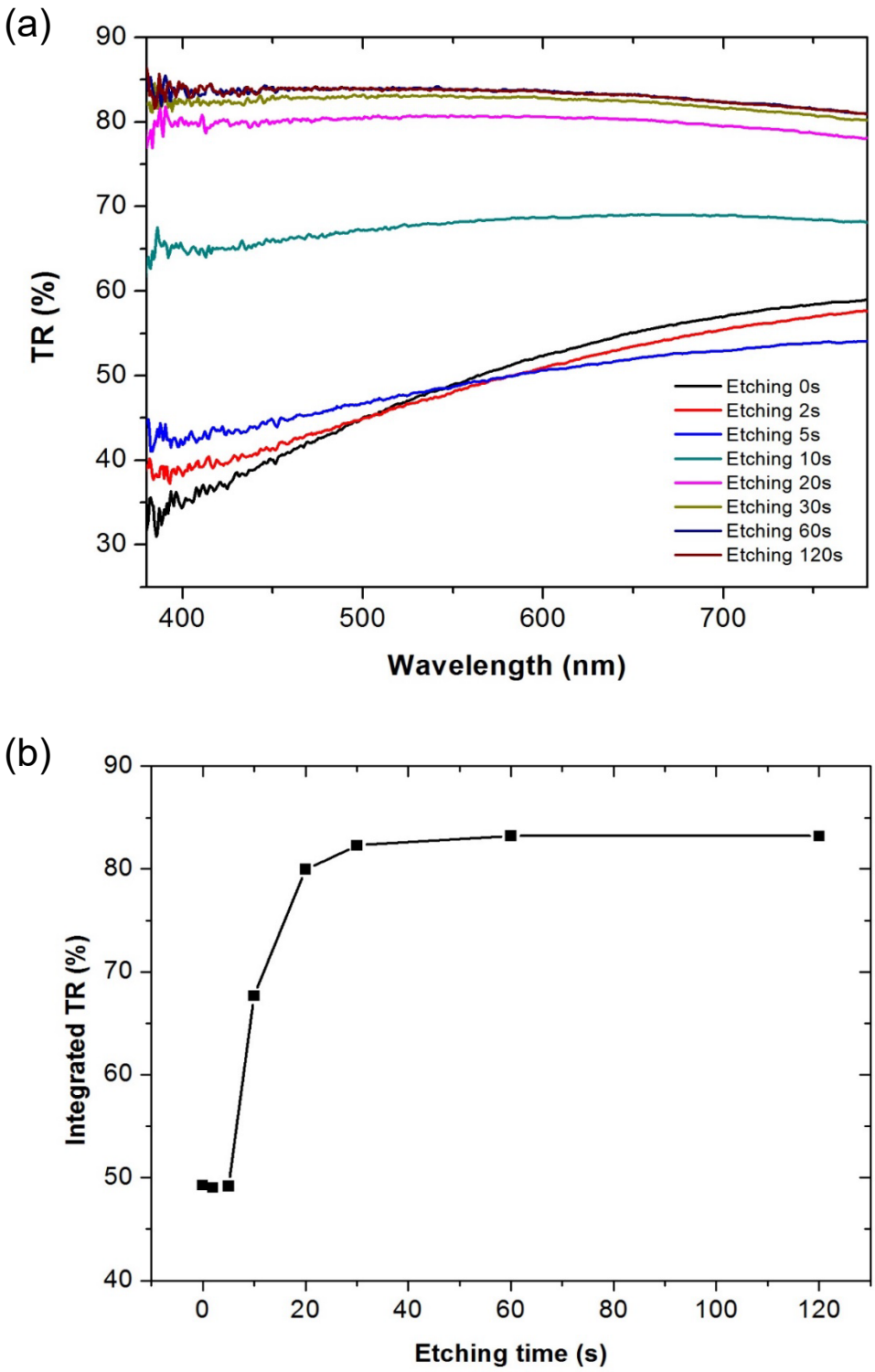

Figure 5. Reflectivity of 1.5mm gauge AA5182-O automotive sheet surface subjected to different level of alkaline etching: (a) surface total reflectance as a function of visible light wavelength; (b) integrated total reflectance as a function of alkaline etching time.

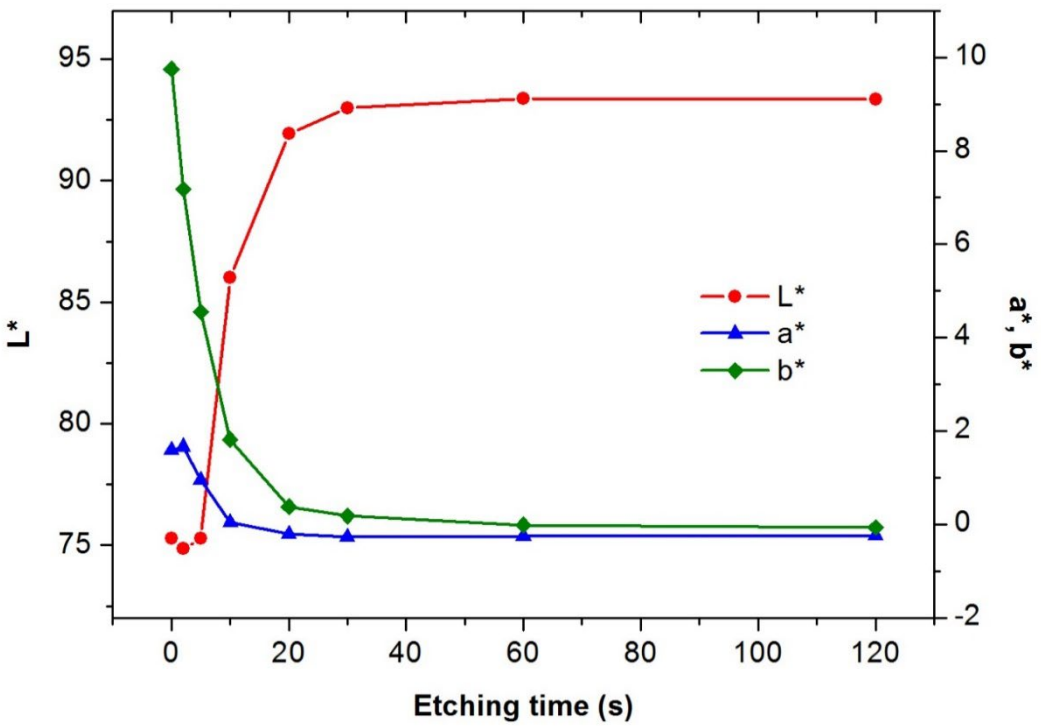

Figure 6. Lightness value L* and chromaticity values a* and b* of 1.5 mm gauge AA5182-O automotive sheet surface as a function of the alkaline etching time.

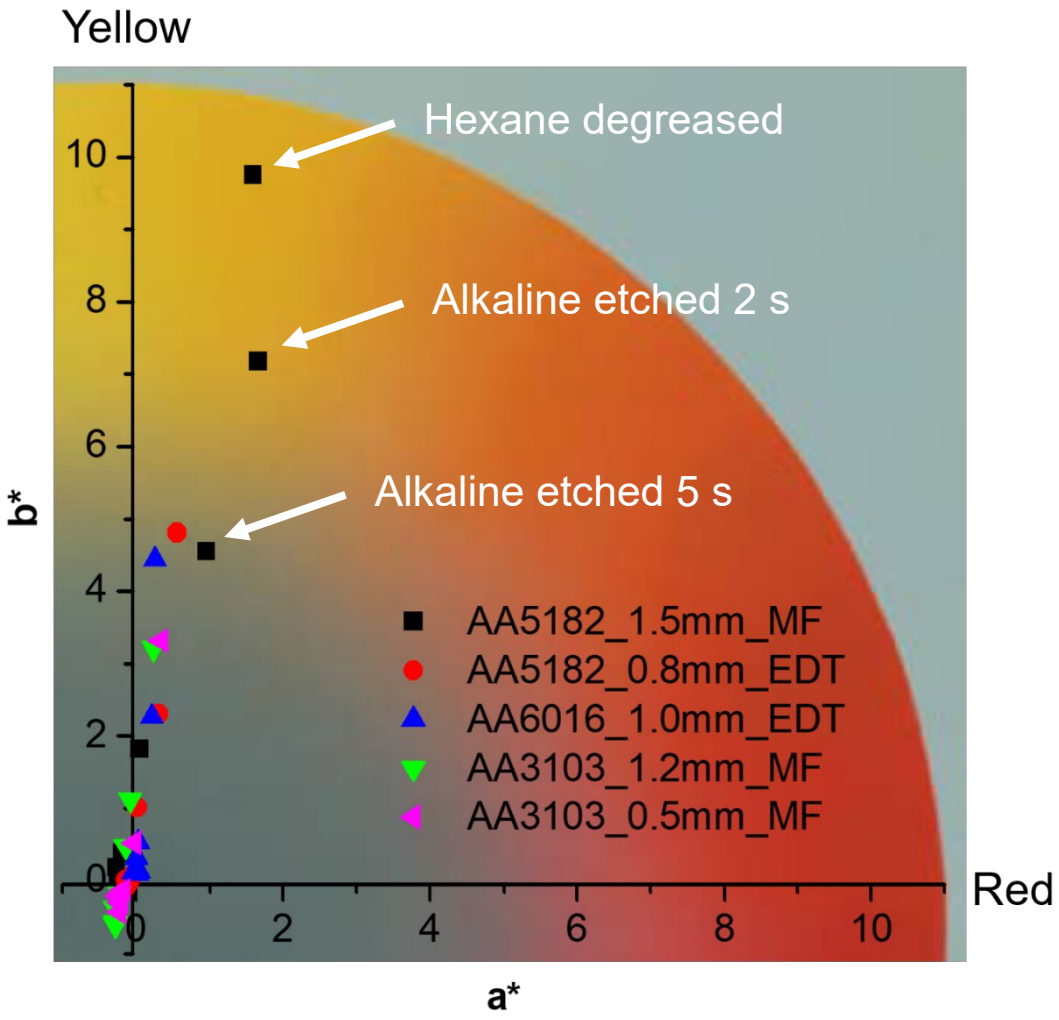

Figure 7. A portion of a*, b* chromaticity diagram with a constant L* value, showing the chromaticity of a variety of aluminium sheet surfaces subjected to different level of cleaning.

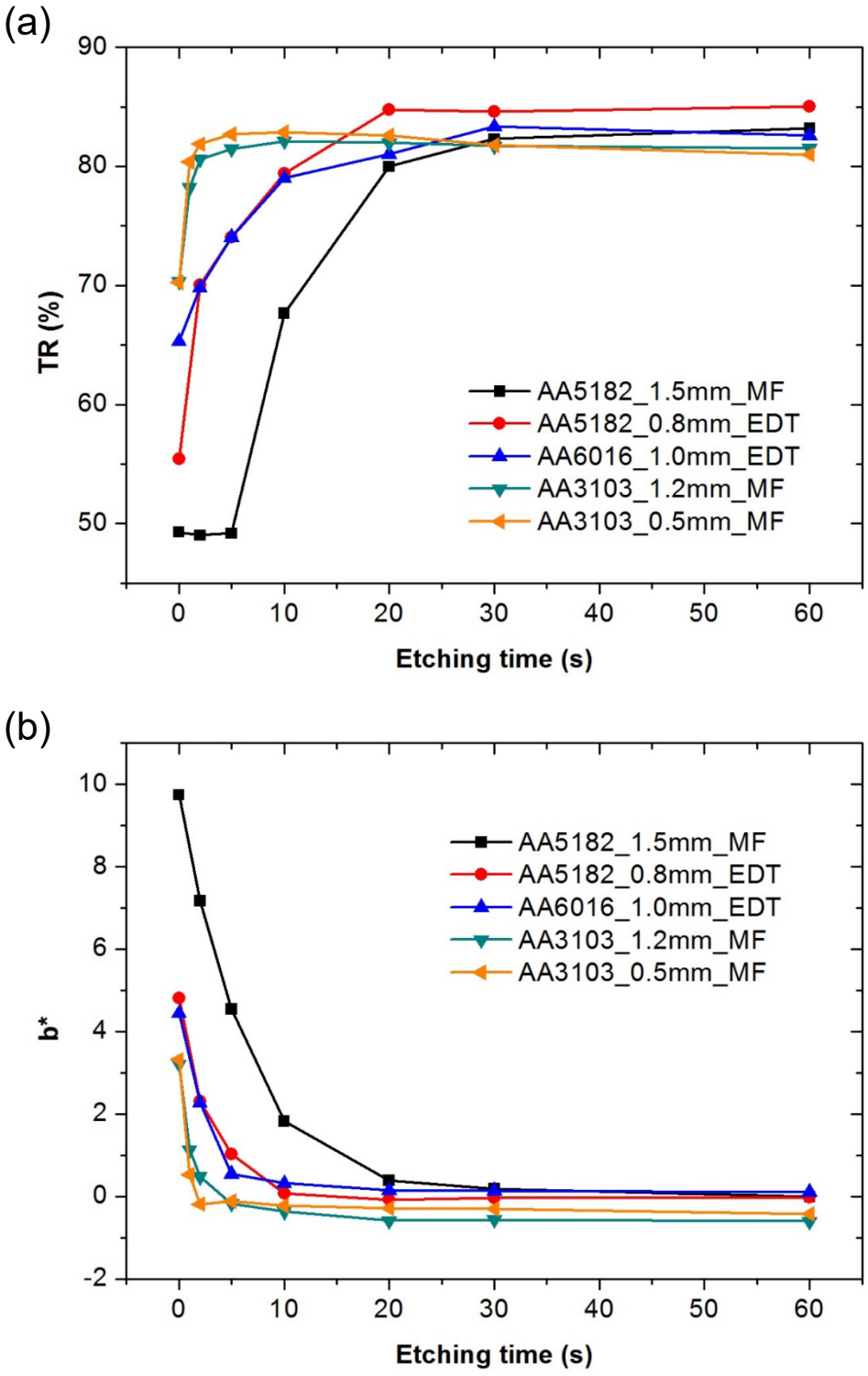

Figure 8. Reflectivity of aluminium alloys subjected to different level of alkaline etching: (a) integrated total reflectance; (b) profiles of chromaticity value b*.